Dynamics of Multidimensional Barrier Crossing in the Overdamped Limit

Benny Carmeli[1], Vladimiro Mujica[2], and Abraham Nitzan[3]

School of Chemistry, Tel-Aviv University, Tel-Aviv 69978, Israel

Chemical Kinetics / Diffusion / Nonequilibrium Phenomena / Transport Properties

Two methods for numerical solution of multidimensional diffusion problems are presented and applied to the two dimensional barrier crossing problem in the overdamped limit. One of these methods is based on evaluating the smallest non-vanishing eigenvalue of the Smoluchowski equation, and the other is based on an adaption of Chandler's steady state correlation function approach. Both methods make use of the fast Fourier transform algorithm for solving a transformed version of the Smoluchowski equation. The numerical solutions are compared to results based on the Kramers theory and some observations concerning effects of the dynamics of barrier crossing problems are made.

1. Introduction

The concept of activated processes provides a common reference framework for the description of numerous important phenomena in chemistry and physics, such as chemical reactions in gaseous and condensed phases, desorption from and diffusion on surfaces, diffusion of atoms and ions inside solids, dynamics of Josephson junctions and others [1]. The Smoluchowski equation has been widely used for describing these and other kind of relaxation processes [2] in the overdamped (high friction) regime. In the one dimensional case it takes the following form

$$\frac{\partial}{\partial t} P(x,t|x') = D \frac{\partial}{\partial x}\left[\frac{\partial}{\partial x} + \beta \frac{\mathrm{d}V(x)}{\mathrm{d}x}\right] P(x,t|x') \qquad (1)$$

where $P(x,t|x')$ is the probability density for finding the system at position x at time t given that it has been initially at x', $D = k_B T/\gamma M$ is the diffusion constant (k_B is the Boltzman constant, T is the absolute temperature, γ denotes the friction coefficient and M is the mass of the diffusing particle), β is the inverse of $k_B T$ and $V(x)$ is the potential of mean force. While one dimensional models are frequently useful to describe the evolution of a system along the reaction coordinate (namely the minimum energy path between the initial and final states) motion in directions normal to the reaction coordinate may have significant dynamic consequences [2–13].

In this paper we discuss methods for the numerical solution of the multidimensional analog of Eq. (1), and apply two such methods to a two dimensional barrier crossing problem. Multidimensional effects on the dynamics of barrier crossing processes have been subjects of several studies lately [2–12]. Several issues, such as the effect of diffusion in directions other then the reaction coordinate, the effect of curvature of the reaction coordinate and the effect of non-isotropic diffusion, are of interest. A numerical algorithm based on the use of fast Fourier transform (FFT) for solving the diffusion equation was recently presented by Agmon and Kosloff [12]. Approximate methods based on time dependent self consistent field approximations were investigated by Kaufman and Whaley [14]. In the present work we describe an improved FFT method, where by transforming the original Smoluchowski equation to a Schrödinger-like equation (eliminating the first order spatial derivatives) we are able to use the analog of the Fleck and Feit split order propagation scheme [15] rather than the finite difference method of Kosloff and Kosloff [16]. Moreover, we focus on the barrier crossing rate, and apply the numerical technique to directly evaluate theoretically based expressions for this rate rather than trying to extract it from the resulting time evolution. Finally we use our results to discuss several issues associated with barrier crossing problems as mentioned above.

Section (2) of this paper describes the numerical method. Section (3) describes the application of the numerical approach to the calculation of the rate by solving for the smallest non-vanishing eigenvalue of the Smoluchowski equation and by evaluating the saturation-plateau value of $\langle N(0)\dot{N}(t)\rangle$ where $N(t)$ is the population in the reactant well at time t. Application to a particular two dimensional model is described in Section (4). Section (5) presents and discusses the numerical results for a model two dimensional system. We conclude in Section (6).

2. Numerical Solution of the Diffusion Equation

The multidimensional version of the diffusion equation (Eq. (1)) is

$$\frac{\partial}{\partial t} P(\boldsymbol{x},t|\boldsymbol{x}') = \nabla^T \cdot \mathbf{D} \cdot [\nabla + \nabla(\beta V(\boldsymbol{x}))]\, P(\boldsymbol{x},t|\boldsymbol{x}') \qquad (2)$$

where $\boldsymbol{x}$ denotes a vector in the multidimensional configuration space and $\mathbf{D}$ is the multidimensional diffusion tensor.

[1] Present address: Department of Physics, Nuclear Research Centre – Negev, P.O. Box 9001, Beer-Sheva 84190, Israel.
[2] Present address: Escula de Quimica, Facultad de Ciencias, Universidad Central de Venezuela, Apartado 47102, Caracas 1051, Venezuela.
[3] Present address: Chemical Physics Department, Weizmann Institute of Science, Rehovot 76100, Israel.

  0005-9021/91/0303-0319 $ 3.50+.25/0

$\mathbf{D}$ is assumed to be constant (namely independent of position) but not necessarily isotropic.

A formal solution to Eq. (2) is

$$P(x,t|x') = \exp(\mathbf{L}t)\cdot P(x,t=0|x') \tag{3}$$

where

$$\mathbf{L} = \nabla^T\cdot\mathbf{D}\cdot[\nabla+\nabla(\beta V(x))] . \tag{4}$$

An exact solution to Eq. (2) cannot be obtained in the general case. The FFT method for solving time dependent problems associated with linear partial differential equations has been recently shown by Agmon and Kosloff [12] to be very useful for solving the Smoluchowski equation. The simplest time propagation procedure is based on a first order difference scheme, namely

$$P(x,t+\Delta t|x') = P(x,t|x')+\Delta t\mathbf{L}P(x,t|x')+O(\Delta t^2). \tag{5}$$

The 2nd order scheme used for Schrödinger equation is not stable in the present case. Agmon and Kosloff [12] have used an expansion of the evolution operator in Chebychev polinomials [16b]. Another convenient algorithm can be obtained in principle by working with the exponential propagator defined in Eq. (3), in the spirit of the split operator method of Feit and Fleck [15]. However since the operator $\mathbf{L}$ contains coupling between x and ∇ it is not possible to split $\exp(\mathbf{L}\Delta t)$ (for small Δt) into a product of exponentials which depend either on x or on $\partial/\partial x$ as is done in the quantum mechanical case.

There exist a transformation [17], which allows to decouple the position from the gradient operators, thus making it possible to use the exponential propagator without the need to linearize it. Let $P_e(x)$ denote the equilibrium solution of Eq. (2) and define

$$\Phi(x,t|x') = \frac{P(x,t|x')}{\sqrt{P_e(x)}} . \tag{6}$$

Then it is easy to show that the function Φ satisfies a Schrödinger like equation

$$\frac{\partial}{\partial t}\Phi = -\mathbf{H}\Phi \tag{7}$$

where the "Hamiltonian" H is

$$\mathbf{H} = -\nabla^T\cdot\mathbf{D}\cdot\nabla + U(x) \tag{8}$$

and the "effective potential" U is

$$U(x) = \nabla^T(\beta V/2)\cdot\mathbf{D}\cdot\nabla(\beta V/2) - \nabla^t\cdot\mathbf{D}\cdot\nabla(\beta V/2) . \tag{9}$$

To obtain these results it has been assumed that the diffusion tensor is symmetric (i.e., $\mathbf{D} = \mathbf{D}^T$).

Let $\{\varphi_n(x)\}$ and $\{\lambda_n\}$ respectively denote the sets of (normalized) eigenfunctions and eigenvalues of $\mathbf{H}$. The Green's function associated with Eq. (7) is given by

$$\Phi(x,t|x') = \sum_{n=0}^{\infty}\varphi_n(x)\cdot\exp(-\lambda_n t)\cdot\varphi_n(x') . \tag{10}$$

Since $\mathbf{H}$ is real and symmetric its left eigenfunctions are identical to its right eigenfunctions $\varphi_n(x)\equiv\langle n|x\rangle = \langle x|n\rangle$. This is in contrast to the operator $\mathbf{L}$ whose right and left eigenfunctions are not identical. Denoting the latter by $\psi_n(x)$ and $\psi_n^+(x)$ we have

$$\psi_n(x) = \varphi_n(x)\cdot\sqrt{P_e(x)} \tag{11a}$$

$$\psi_n^+(x) = \varphi_n(x)/\sqrt{P_e(x)} . \tag{11b}$$

The corresponding eigenvalues are identical to those of $\mathbf{H}$ and satisfy

$$\lambda_n = \langle\varphi_n(x)|\mathbf{H}|\varphi_n(x)\rangle = \langle\psi_n(x)|\mathbf{L}|\psi_n(x)\rangle \geq 0 . \tag{12}$$

Assuming that the "ground state" $\varphi_0(x)$ is nondegenerate, only one of the eigenvalues, λ_0, is zero and all the others are positive. The normalization condition implies

$$\int_{-\infty}^{\infty} dx^{(N)}\varphi_0(x)\cdot\Phi(x,t|x') = \int_{-\infty}^{\infty} dx^{(N)}\Phi(x,t|x')\cdot\varphi_0(x') = 1 \tag{13}$$

where N is the dimensionality.

The problem of solving Eq. (2) has thus been transformed into that of solving Eq. (7) where the "momentum" terms (the terms containing ∇) and those depending on position are separated. Note that this simple form for the "Hamiltonian" (Eq. (8)) is obtained only for position-independent diffusion tensors.

The time evolution associated with Eq. (7) is obtained from

$$\Phi(x,t) = \langle x|\exp(-\mathbf{H}t)|\Phi(t=0)\rangle \approx \langle x|\prod_1^n\exp(-\mathbf{T}\Delta t)\cdot\exp(-\mathbf{U}\Delta t)|\Phi(t=0)\rangle \tag{14}$$

where the "kinetic energy" operator $\mathbf{T}$ denotes the term $-\nabla^T\cdot\mathbf{D}\cdot\nabla$ appearing in Eq. (8) and where $\Delta t = t/n$. In practice, the function Φ is defined on a grid in configuration space. The $\exp(-\mathbf{T}\Delta t)$ operator is carried out by the FFT technique.

$$\Phi(x,\Delta t) \approx F_{x\leftarrow k}[e^{-\mathbf{T}\Delta t}F_{k\leftarrow x}(e^{-\mathbf{U}\Delta t}\Phi(x,0))] \tag{15}$$

where the two exponential operators appear in their diagonal representations in the appropriate space, and where $F_{x\leftarrow k}$ denotes a Fourier transform from k-space to x-space

$$f(x) = F_{x\leftarrow k}\hat{f}(k) = \left(\frac{1}{2\pi}\right)^N\int_0^{2\pi} dk^{(N)}\exp(-ik\cdot x)\hat{f}(k) . \tag{16}$$

The choice of the initial distribution requires some attention. In principle it is possible to make an arbitrary selection but

it is advantageous to do it in such a way that the calculation of the specific observable of interest, e.g., transition rate, is easier. This point is discussed below.

3. The Transition Rate and the Reactive Flux

The type of processes which are considered in this section involve classical diffusion over a barrier, from a potential well to another region of the configuration space. In particular we are interested in the transition rate and in the condition for it to exist as a meaningful measure of the reaction dynamics [17–21].

It is convenient to write Eq. (2) as a continuity equation

$$\partial_t P(\boldsymbol{x},t) + \nabla^T \cdot \boldsymbol{J}(\boldsymbol{x},t) = 0 \tag{17}$$

where the probability flux vector, $\boldsymbol{J}(\boldsymbol{x},t)$ is given by

$$\boldsymbol{J}(\boldsymbol{x},t) = -\mathbf{D} \cdot [\nabla + \nabla(\beta V(\boldsymbol{x}))] P(\boldsymbol{x},t) . \tag{18}$$

At a stationary state $\boldsymbol{J}(\boldsymbol{x},t) = \boldsymbol{J}_s$, is a constant, and $P(\boldsymbol{x},t) = P_s(\boldsymbol{x})$ does not evolve in time. For closed systems the only stationary state is the equilibrium distribution $P_e(\boldsymbol{x})$, for which $\boldsymbol{J}_e = 0$. The barrier crossing process is characterized by a single rate (for practical purposes) if, following a short transient period after the initiation of the process, the system developes a quasi steady state whose time evolution is governed by the smallest non-vanishing eigenvalue of the Smoluchowski equation and by a nearly constant flux from the reactant to the product well. Several approximate methods to evaluate this steady state rate are available:

(a) The Smallest Non-Vanishing Eigenvalue (SNVE) Method [18, 20]

The existence of a well defined rate implies that λ_1, the smallest non-vanishing eigenvalue of $\mathbf{L}$, is well separated from the higher eigenvalues (i.e., $\lambda_1 \ll (\lambda_2 - \lambda_1) \equiv \tau^{-1}$) and that this eigenvalue is not degenerate. With this in mind and for times t such that $\lambda_2^{-1} \ll t < \infty$ the relaxation to equilibrium is governed by λ_1 which is then equal to the transition rate $K(\beta)$.

These well recognized facts can be used within the numerical scheme described in Sect. (2) as follows: Using an arbitrary initial distribution $\varphi(\boldsymbol{x},0)$ the distribution at time t is obtained by performing the evolution $\varphi(\boldsymbol{x},t) = \mathrm{e}^{-\mathbf{H}t}\varphi(\boldsymbol{x},0)$ numerically. Observing that

$$\theta(\boldsymbol{x},t) = \varphi(\boldsymbol{x},t) - \varphi_0(\boldsymbol{x}) \tag{19}$$

($\varphi_0(\boldsymbol{x})$ is the state corresponding to the eigenvalue $\lambda_0 = 0$) satisfies

$$\|\theta(t)\|^2 \equiv \int_{\infty}^{\infty} \mathrm{d}\boldsymbol{x} |\theta(\boldsymbol{x},t)|^2 = \|\varphi(t)\|^2 - 1 \tag{20}$$

the transition rate $K(\beta)$ is obtained from

$$K(\beta) = -\frac{1}{2} \lim_{t \gg \tau} \frac{\mathrm{d}}{\mathrm{d}t} \ln[\|\varphi(t)\|^2 - 1] . \tag{21}$$

Alternatively, if the initial "wave function" $\varphi(\boldsymbol{x},0)$ does not contain the "ground state" $\varphi_0(\boldsymbol{x})$ i.e., $\langle\varphi_0|\varphi(0)\rangle = 0$, (this may be achieved, since $\varphi_0(\boldsymbol{x})$ is the known equilibrium distribution, by the projection $\varphi(\boldsymbol{x},0) \to \varphi(\boldsymbol{x},0) - \langle\varphi_0(\boldsymbol{x})|\varphi(\boldsymbol{x},0)\rangle$ followed by renormalization) then

$$K(\beta) = \lambda_1 = \lim_{t \gg \tau} \frac{\mathrm{d}}{\mathrm{d}t} \ln[\|\varphi(t)\|) . \tag{22}$$

(b) Chandler's Method [21]

A different treatment for the calculation of the transition rate is based on the fluctuation dissipation theorem. Close to equilibrium the relaxation process of an observable $A(t)$ obeys the following relation

$$\frac{\langle \delta A(t)\rangle_{\mathrm{ne}}}{\langle \delta A(0)\rangle_{\mathrm{ne}}} = \frac{\langle \delta A(0)\, \delta A(t)\rangle}{\langle \delta A(0)^2\rangle} . \tag{23}$$

Where $\langle\cdots\rangle$ and $\langle\cdots\rangle_{\mathrm{ne}}$ respectively represent an equilibrium ensemble average (over initial conditions) and a non-equilibrium one, and $\delta A(t) = A(t) - \langle A\rangle$.

The observable of interest is

$$N(t) = \int_{\Omega} \mathrm{d}\boldsymbol{x}\, P(\boldsymbol{x},t|\boldsymbol{x}_0) \tag{24}$$

where Ω is the domain defining the reactant state and $P(\boldsymbol{x},t|\boldsymbol{x}_0)$ is the distribution at time t given that initially it was

$$P(\boldsymbol{x},t=0|\boldsymbol{x}_0) = \delta(\boldsymbol{x} - \boldsymbol{x}_0) ; \quad \boldsymbol{x}_0 \in \Omega \tag{25}$$

where x_i is the i-th component of the N-dimensional vector $\boldsymbol{x}$ and x_{i0} is the initial location of the distribution on the i-th coordinate axis. The reaction coordinate is the minimum energy path between the reactants and the products potential wells. However dynamical effects may create situations in which the maximum reactive flux does not go along the minimum energy path. This aspect of the problem will be discussed below in the specific application to two-dimensional diffusion. Define

$$\delta N(t) = \int_{\Omega} \mathrm{d}\boldsymbol{x} [P(\boldsymbol{x},t|\boldsymbol{x}_0) - \mathrm{e}^{-\beta V(\boldsymbol{x})}/Q] \tag{26a}$$

where

$$Q = \int_{-\infty}^{\infty} \mathrm{d}\boldsymbol{x}\, \mathrm{e}^{-\beta V(\boldsymbol{x})} . \tag{26b}$$

Assuming that the relaxation of $\langle\delta N(t)\rangle$ to its equilibrium value (i.e., zero) is given by the chemical rate $K(\beta)$, we find from Eq. (23)

$$\langle \delta N(0)\, \delta N(t)\rangle = \langle[\delta N(0)]^2\rangle \exp(-K(\beta)t) \tag{27}$$

and consequently

$$\langle \delta N(0)\, \delta \dot{N}(t)\rangle = -K(\beta)\, \langle[\delta N(0)]^2\rangle \exp(-K(\beta)t) . \tag{28}$$

As discussed above (see also Ref. [21]) for the process at hand to have a uniquely defined rate constant one must consider times such that $\tau \ll t \ll K^{-1}$. Then Eq. (28) implies

$$K(\beta) = \xrightarrow[\tau \ll t \ll K^{-1}]{} - \frac{\langle \delta N(0)\, \delta \dot{N}(t) \rangle}{\langle [\delta N(0)]^2 \rangle}. \tag{29}$$

Thus, evaluating the saturation or plateau value of the r.h.s. of Eq. (29) (using the numerical procedure of Sect. (2) for the numerator) yields $K(\beta)$. It is obvious that apart from reasons of numerical accuracy, the procedures based on Eqs. (20), (21) and (29) should yield identical results.

(c) Kramer's Formula [22]

Kramers has derived an expression for the escape rate out of a one dimensional potential well in several limits associated with the magnitude of the friction. For the overdamped limit governed by the Smoluchowski equation (1) and for high barriers ($E_B \gg k_B T$) his result for the rate is

$$K_{KR}^{(1D)} = \frac{\omega_r^{(B)}\, \omega_r^{(W)}}{2\pi\gamma} \exp\left(-\frac{E_B}{k_B T}\right) \tag{30}$$

where $\omega_r^{(B)}$ and $\omega_r^{(W)}$ are the vibrational frequencies corresponding to the top of the barrier and to the bottom of the well respectively and where the potential in these two regions has been approximated by its expansion up to quadratic terms about these points. For a multidimensional system, Eq. (30) can be generalized by assuming that the nonreactive modes are in thermal equilibrium. Under this assumption the rate takes the form [23]

$$K_{KR}^{(ND)} = \frac{\omega_r^{(B)}}{\gamma} K_{TST}^{(ND)} \tag{31}$$

where ND stands for "N-Dimensional" and where K_{TST} is the rate obtained from transition state theory

$$K_{TST} = \sqrt{\frac{2k_B T}{\pi M}} \frac{\int d\boldsymbol{x}_{nr}\, e^{-\beta V(x_r = x_b)}}{\int dx_r \int d\boldsymbol{x}_{nr}\, e^{-\beta V(x)}}. \tag{32}$$

In Eqs. (31) and (32) the subscripts r and nr stand for reactive and nonreactive coordinates respectively.

4. A Two Dimensional Model

The method described in Sect. (2) has been applied to solve numerically the diffusion equation in two dimensions, to compare the Kramers expression (31)) to different numerical ways of evaluating the rate and to examine effects of multidimensionality on the reaction rates other then these incorporated in Eqs. (31) and (32). The potential surface used in this study may be written in the form

$$V(x,y) = V_0 \cdot f_R(x,y)\, f_L(x,y) \tag{33}$$

where $f(x,y)$ is a quadratic form in x and in y such that $f(x,y) = 0$ describes the locus of an ellipse. In terms of the geometrical parameters defined in Fig. 1, $f(x,y)$ is

$$\begin{aligned} f(x,y) = {} & \left(\frac{x - x_0}{a}\right)^2 [\cos^2(\theta) + \alpha \sin^2(\theta)] \\ & + \frac{x - x_0}{a} \cdot \frac{y - y_0}{a} (1 - \alpha) \sin(2\theta) \\ & + \left(\frac{y - y_0}{a}\right)^2 [\sin^2(\theta) + \alpha \cos^2(\theta)] - 1 \end{aligned} \tag{34}$$

where $(x_0; y_0)$, a, θ and α represent the parameters of any of the two ellipses $f(x,y) = 0$. The subscripts R and L (Right and Left) represent different choices of the parameters. These parameters are chosen for the two ellipses such that the saddle point of the potential is at the origin. For the sake of simplicity we have considered in this article only potentials which are symmetric with respect to the y axis. The parameter V_0 is the hight of the potential barrier and the reaction coordinate i.e., the minimum energy path, goes from one well to the other through the origin. In all the calculations described below we have taken $a_R = a_L = a$, and have chosen the units of time and length such that $a = D_x + D_y = 1$.

In the numerical evaluation of the rate Eq. (22) can be used as written, but Eqs. (28) and (29) may be simplified for the model considered. The dividing surface s, where the flux is calculated, is taken as the y axis. By using the symmetry of the potential $V(x,y)$ with respect to this axis, Eqs. (24), (25) and (2) lead to

$$\begin{aligned} \delta N(t=0) &= \int_0^\infty dx \int_{-\infty}^\infty dy [\delta(x - x_0) \cdot \delta(y - y_0) - e^{-\beta V(x)}/Q] \\ &= \Theta(x_0) - \frac{1}{2} \end{aligned} \tag{35}$$

where $\Theta(x)$ is the Heaviside function. Also from Eq. (2)

$$\begin{aligned} \delta \dot{N}(t) = {} & -D_x \int_{-\infty}^\infty dy \left(\frac{\partial}{\partial x} + \beta \frac{\partial V(x,y)}{\partial x}\right) \\ & \cdot P(x,y,t|x_0,y_0) \end{aligned} \tag{36}$$

$$\begin{aligned} -\langle \delta N\, \delta \dot{N}(t) \rangle = {} & \frac{D_x}{Q} \int_{-\infty}^\infty dy e^{-\beta V(0,y)} \frac{\partial}{\partial x} \\ & \cdot \int_{-\infty}^\infty dx_0 \int_{-\infty}^\infty dy_0 e^{\beta V(x,y)} \\ & \cdot P(x,y,t|x_0,y_0) e^{-\beta V(x_0,y_0)} \left[\Theta(x_0) - \frac{1}{2}\right]\Big|_{x=0}. \end{aligned} \tag{37}$$

Defining

$$\hat{P}(x,y) = e^{-\beta V(x,y)} \left[\Theta(x) - \frac{1}{2}\right]/Q. \tag{38}$$

Eq. (37) takes the form

$$\begin{aligned} -\langle \delta N\, \delta \dot{N}(t) \rangle = {} & D_x \int_{-\infty}^\infty dy\, e^{-\beta V(0,y)} \frac{\partial}{\partial x} \\ & \cdot e^{+\beta V(x,y)} P(x,y,t|\hat{P})]|_{x=0} \end{aligned} \tag{39}$$

where

$$P(x,y,t|\hat{P}) = \int_{-\infty}^{\infty} dx_0 \int_{-\infty}^{\infty} dy_0\, P(x,y,t|x_0,y_0) \cdot \hat{P}(x^0,y^0) = e^{\mathbf{L}t}\hat{P}. \tag{40}$$

Eqs. (39) and (40) imply that the calculation of $\langle \delta N \delta \dot{N}(t)\rangle$ (hence of the escape rate, Eq. (29)) can be done by simply propagating the initial "distribution" $\hat{P}(x,y)$ of Eq. (38). This propagation is performed using the FFT algorithm and the equivalent Schrödinger equation (see below). A final FFT procedure is then used to get the derivative with respect to x in Eq. (39). The evaluation of Eq. (29) is facilitated by noting that the symmetry of the potential implies

$$\langle [\delta N(0)]^2\rangle = \frac{1}{4}. \tag{41}$$

Note that $\hat{P}(x,y)$ can be negative (in fact $\int dx\, \hat{P}(x,y) = 0$) hence it is not a real distribution. An initial real normalized distribution can be constructed as

$$P(x,y,t=0) = P_e(x,y) + \hat{P}(x,y) \tag{42}$$

where $P_e(x,y)$ is the equilibrium distribution. Note that P_e is orthogonal to $\hat{P}$, $\langle P_e|\hat{P}\rangle = 0$; ($\langle P_e| =$ constant). If this choice of initial distribution is made than $\hat{P}$ can be interpreted as the deviation of the initial distribution from equilibrium. In fact it is easy to see that $P(x_0,y_0,t=0)$ can be used in the r.h.s. of Eq. (40) instead of $\hat{P}(x_0,x_0)$ without changing the results for $\langle \delta N \delta \dot{N}(t)\rangle$ in Eq. (37).

In actual calculation we use the language of the equivalent Schrödinger equation to compute the r.h.s. of Eq. (39). The rate Eq. (29) is the given by

$$K = \lim_{\tau \ll t \ll K^{-1}} \frac{4D_x}{Q^{1/2}} \int_{-\infty}^{\infty} dy\, e^{-\beta V(0,y)} \frac{\partial}{\partial x} \cdot [e^{+\beta V(x,y)} \Phi(x,y,t|\hat{\Phi})|_{x=0}] \tag{43}$$

where $\Phi(x,y,t|\hat{\Phi})$ is defined in analogy with Eq. (40) as the "wave function" at time t, given that at $t=0$ it was

$$\hat{\Phi}(x_0,y_0) = \varphi_0(x_0,y_0)\left[\Theta(x_0) - \frac{1}{2}\right]. \tag{44}$$

It is evaluated as $\Phi(x,y,t|\hat{\Phi}) = e^{-\mathbf{H}t}\hat{\Phi}$. Note that by symmetry it is orthogonal to the "ground state" $\varphi_0(x,y)$ at all time.

Next consider the Kramers result in two dimensions. Eq. (31) takes the form

$$K_{KR}^{(2D)} = \frac{\omega_r^{(B)}}{\gamma} K_{TST}^{(2D)} \tag{45}$$

where γ is given by

$$\gamma = \frac{k_B T}{D_x M} \tag{46}$$

and where

$$K_{TST}^{(2D)} = A\sqrt{\frac{2k_B T}{\pi M}} \tag{47}$$

with

$$A = \frac{\int_{-\infty}^{\infty} dy\, e^{-\beta V(0,y)}}{\int_{-\infty}^{\infty} dx \int_{-\infty}^{\infty} dy\, e^{-\beta V(x,y)}}. \tag{48}$$

Since the origin is at the saddle point the barrier frequency is obtained from

$$\left.\frac{\partial^2 V}{\partial x^2}\right|_{x=0,\,y=0} = -M(\omega_r^{(B)})^2. \tag{49}$$

Substitution of Eqs. (47) and (48) in (45) then leads to

$$K_{TST}^{(2D)} = D_x A \sqrt{-\frac{2\beta}{\pi}\left.\frac{\partial^2 V}{\partial x^2}\right|_{x=0,\,y=0}}. \tag{50}$$

5. Results and Discussion

The initial "distribution" used in our calculation is given by Eq. (38). This corresponds to the actual distribution Eq. (42), leading to

$$P_R = \int_0^{\infty} dx \int_{-\infty}^{\infty} dx\, P(x,y,0) = \frac{3}{4} \tag{51a}$$

and

$$P_L = \int_{\infty}^{0} dx \int_{-\infty}^{\infty} dx\, P(x,y,0) = \frac{1}{4}. \tag{51b}$$

Eqs. (51a) and (51b) imply that the diffusion process following the preparation of this initial state proceeds from right to left.

In Table 2 we present results obtained from the different methods described in the previous sections: The smallest eigenvalue (SNVE) method (Eq. (22)), Chandler's steady state relaxation rate (CSSR) method (Eqs. (29) and (43)) and the Kramers' steady state rate (KSSR Eq. (50)). These results are given for different choices of the model parameters given in Table 1. All the calculations where performed on a $2^7 \times 2^7$ grid covering the physical dimensions $x = (-1.5;1.5)$, $y = (-1.0,1.0)$ (hence the spacings are $\Delta x = 1.5 \times 2^{-6}$ $\Delta y = 1.0 \times 2^{-6}$). The parameters in Table 1 characterize the potential surface and the diffusion rates. The last colomn in Table 2 gives the number of timesteps used in the numerical time evolution.

Two of the potential surfaces used in the calculations described here are shown in Figs. 2 and 3. These figures display the potential surfaces corresponding to cases 1 (also 3 and 4) and 9 (also 11 and 12) of Table 1 respectively. Cases 1–4

Table 1
Description of cases

Potential parameters*)	D_x/D_y	βV_0	Case
$\theta_L = 0$	1.0	6	1
$\theta_R = 0$	1.0	2	2
$\theta_S = \pi/2$	5.0	6	3
$\alpha_L = 5.0$	0.2	6	4
$\alpha_R = 5.0$			
$\tau = 1$			
$\theta_L = \pi/3$	1.0	6	5
$\theta_R = \pi/6$	1.0	2	6
$\theta_S = \pi/2$	5.0	6	7
$\alpha_L = 0.2$	0.2	6	8
$\alpha_R = 5.0$			
$\tau = 1$			
$\theta_L = \pi/4$	1.0	6	9
$\theta_R = \pi/4$	1.0	2	10
$\theta_S = \pi/2$	5.0	6	11
$\alpha_L = 0.2$	0.2	6	12
$\alpha_R = 5.0$			
$\tau = 1$			

*) See Fig. 1.

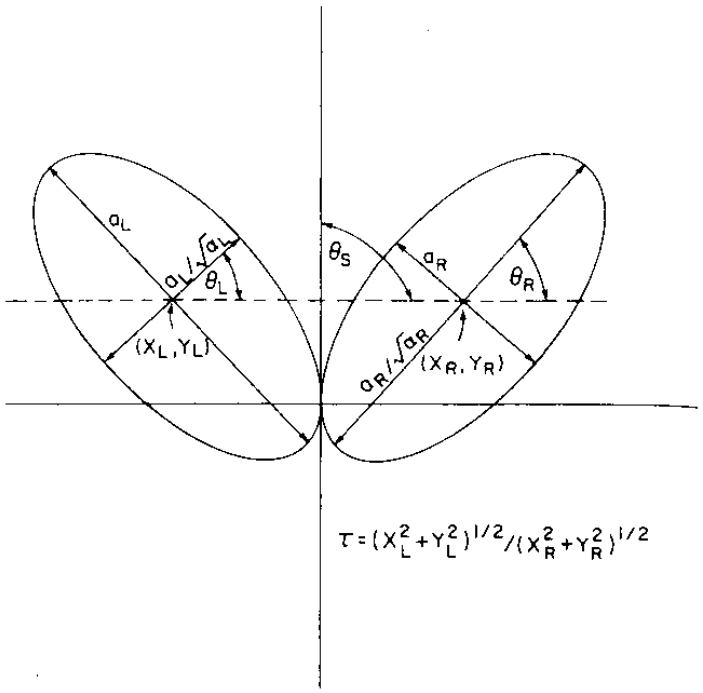

Fig. 1
Description of the geometrical parameters of the potential, Eq. (33). θ_S is the angle between the two principal axes of the diffusion tensor. In all the present calculations $\theta_S = \pi/2$ and these two principal axes are taken as the cartesian axes x and y

Table 2
Transition rates

Case	SNVE[1]	CSSR[1]	KSSR[3]	Time
1	0.05007	0.05027	0.05658	2000
2	0.70500	0.69150	0.69950	2000
3	0.08379	0.08260	–	2000
4	0.01449	0.01775	–	2000
5	0.05123	0.05156	0.05616	2000
6	0.70290	0.60090	0.59740	2000
7	0.07191	0.07252	–	2000
8	0.01774	0.02086	–	2000
9	0.04751	0.04853	0.05677	2000
	0.04742	0.04712	–	3000
10	0.69200	0.59080	0.57210	2000
	0.67330	0.50260	–	3000
11	0.06221	0.06521	–	2000
	0.06170	0.06214	–	3000
12	0.01870	0.02101	–	2000
	0.01833	0.01942	–	3000

[1] SNVE: Smallest Non-Vanishing Eigenvalue method, Eq. (22).
[3] CSSR: Chandler's Steady State relaxation Rate, Eq. (43).
[3] KSSR: Kramer's Steady State relaxation Rate, Eq. (45).

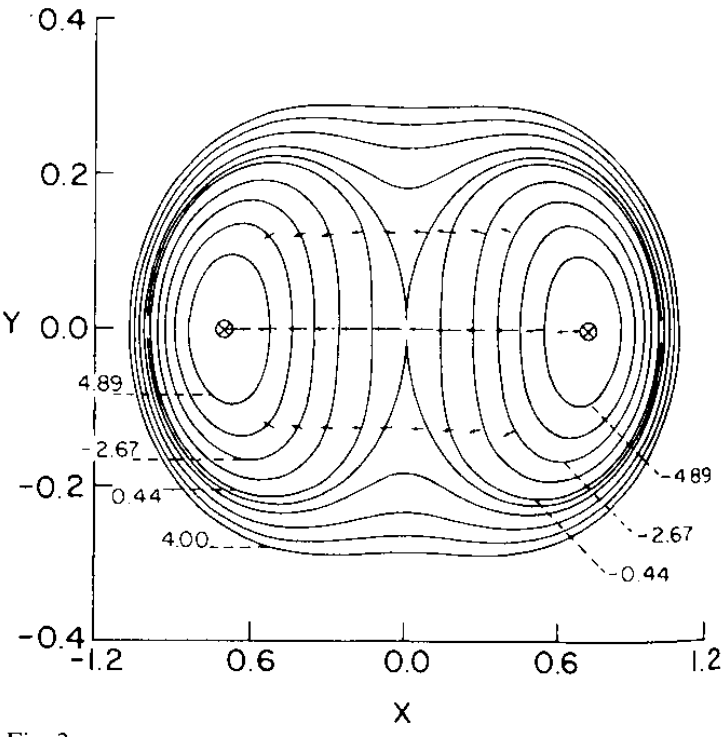

Fig. 2
Contour plot of the potential energy surface of case 3 with arrows indicating the direction and magnitude of the steady state reactive flux

correspond to a linear reaction coordinate while cases 5–8 and 9–12 represent two groups of situations with curved reaction coordinate. Some of the cases (2,6 and 10) correspond to a small barrier hight ($\beta V_0 = 2$) where the experimental reaction rate is not well defined. For the other cases $\beta V_0 = 6$. Finally in cases 1,2,5,6, and 9,10 the diffusion tensor is isotropic while the other cases correspond to non isotropic diffusion.

From Table 2 we see that good agreement between the two numerical procedures considered in this paper exists in all cases where the rate is well defined (discrepancies are of the same order as the numerical accuracy of the results). It should be noted that the numerical accuracy is also considerably better for the high potential barrier cases where the smallest non-vanishing eigenvalue is well separated from the higher eigenvalues (or where the saturation region in Eq. (29) is well defined). In these cases we have found that at time 2000 (time units correspond to $a = D_x + D_y = 1$)

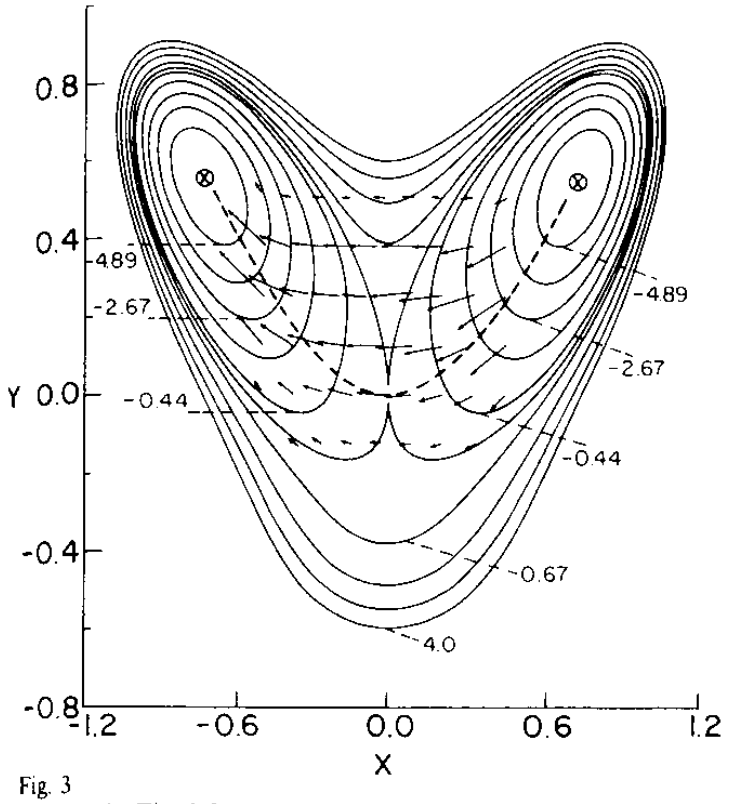

Fig. 3
Same as in Fig. 2 for case 11

the error was less than 3%. The Kramers result also works reasonably well when applied to the isotropic cases (in fact its success for cases 2,6 and 10 ($\beta V_0 = 2$) is surprising, and is probably fortuitous.

Consider now the effect of curvature on the reaction coordinate and of anisotropy on the diffusion tensor. These issues have been recently subjects of several studies. A recent study [6] of the effect of the reaction path curvature in the overdamped (Smoluchowski) limit of the Kramers problem has shown that for isotropic diffusion (and isotropic potential wells) the curvature of the reaction coordinate plays no direct role in the reaction kinetics, as is intuitively clear since this kinetics is dominated by the flux across the saddle point. Still Matkowsky et al. [6] have shown that the pre-exponential factor in the reaction rate may be modified by the diffusion in direction(s) normal to the reaction coordinate, and thus may account for part of the difference between the result based on the (essentially one dimensional) Kramers expression and the numerical work. (Note that the Kramers result is the lowest order term in an expansion in powers of $(\beta V_0)^{-1}$, so corrections are expected even in one dimension).

Of more interest is the effect of non isotropic diffusion, particularly when the reaction coordinate does not coincide with a principal axis of the diffusion tensor. (Cases 3 and 4 correspond to situations when it does). Kłosek et al. [8,9], as well Berezhkovskii and Zitserman [10,11] have shown that a qualitative difference exists between the cases where the second derivative A of the potential at the saddle point in the direction of fast diffusion is larger or smaller than zero. When $A > 0$ the large potential barrier and large diffusion anisotropy are interchangable, and a trivial generalization of the Kramers problem applies. When $A < 0$ the situation is much more complicated. We defer a detailed

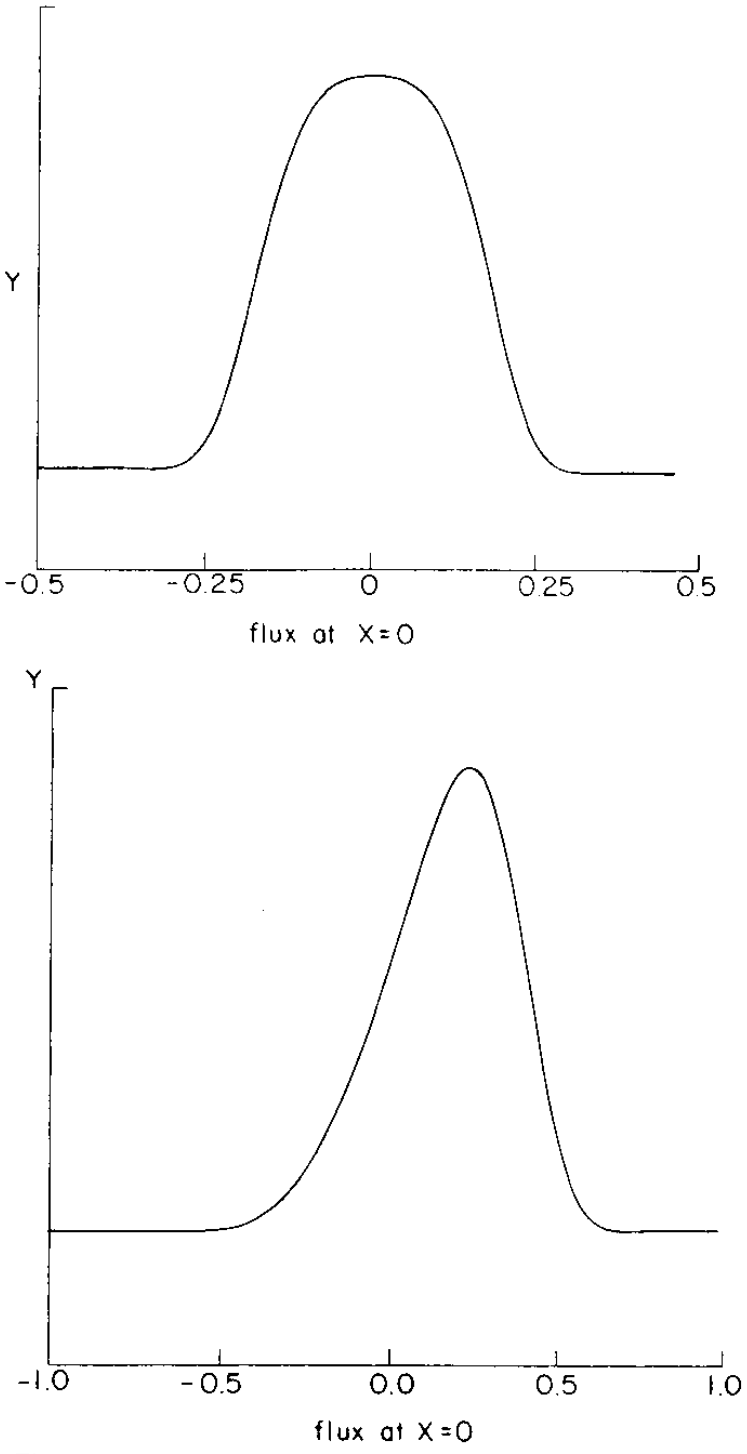

Fig. 4
The reactive flux along the y axis, at $x = 0$ vs. position.
(a) case 3; (b) case 11

comparison between the analysis of this situation and the numerical work to a later publication. Here we note that this case correspond to $D_x > D_y$ (cases 3, 7 and 11) and is characterized here by the fact that the reactive flux across the ridge ($y = 0$) between the two wells is not necessarily the largest at the saddle point. To see this we have plotted in Figs. 2 and 3, superimposed on the potential surfaces corresponding to cases 1(3,4) and 9(11,12) respectively, arrows whose direction and length represent the direction and magnitude of the reaction flux. The latter is obtained from

$$J_x(x,y,t) = -D_x\left[\frac{\partial}{\partial x} + \beta\frac{\partial V(x,y)}{\partial x}\right]P(x,y,t) \tag{52}$$

$$J_y(x,y,t) = -D_y\left[\frac{\partial}{\partial y} + \beta\frac{\partial V(x,y)}{\partial y}\right]P(x,y,t) \tag{53}$$

where $P(x,y,t)$ is taken at the quasi-stationary state for which the transition rate is calculated. The flux arrows in Fig. 2 correspond to case 3 and the flux arrows in Fig. 3 — to case 11. The length $l(x,y)$ of an arrow at location (x,y) is taken as

$$l(x,y) = p\cdot\left[\left(\frac{\partial J}{\partial x}\right)^2 + \left(\frac{\partial J}{\partial y}\right)^2\right]^{1/2} \tag{54}$$

where p is an arbitrary scale factor.Fig. 3 clearly shows the deviation of the maximal flux from the geometrical saddle point. This deviation depends on the geometry of the potential surface, on the diffusion anisotropy and on the temperature, and may lead to non-Arrhenius temperature dependence of the reaction rate. Another view of the same effect is shown in Fig. 4, where we plotted the x component of the reactive flux as a function of the position y along the y axis ($x = 0$). Shown are plots for case 3 (Fig. 4a) and for case 11 (Fig. 4b). The fact that for the latter case the flux peaks at $y = 0$ (position of the saddle point) clearly demonstrates the effect discussed above.

6. Conclusion

In this paper we have described numerical methods for solving multidimensional diffusion equations and have applied these methods to a model chemical reaction where curved reaction coordinates and anisotropic diffusion play non-trivial role in determining the reaction rate. The appearence of such multidimensional effects even in the relatively simple overdamped situation emphasizes the shortcomings of analyzing reaction rates from equilibrium and dynamical considerations purely at the transition state.

This work has been supported in part by the U.S-Israel Binational Science Foundation and by the Israel Academy of Science. We thank N. Agmon for helpful comments.

References

[1] For a very recent review see P. Hänggi, P. Talkner, and M. Borkovec, Rev. Mod. Phys. *62*, 251 (1990).
[2] N. Agmon and J. J. Hopfield, J. Chem. Phys. *78*, 6947 (1983); ibid. *70*, 2042 (1983); N. Agmon, Biochemistry *27*, 3507 (1988).
[3] R. S. Larson and D. Kostin, J. Chem. Phys. *77*, 5017 (1982).
[4] R. S. Larson , Physica *A 137*, 295 (1986).
[5] R. S. Larson, J. Chem. Phys. *89*, 1291 (1989).
[6] B. J. Matkowsky, A. Nitzan, and Z. Schuss, J. Chem. Phys. *88*, 4765 (1988).
[7] B. J. Matkowsky, A. Nitzan, and Z. Schuss, J. Chem. Phys. *90*, 1292 (1989).
[8] M. M. Kłosek-Dygas, B. M. Hoffman, B. J. Matkowsky, A. Nitzan, M. A. Ratner, and Z. Schuss, J. Chem. Phys. *90*, 1141 (1989).
[9] M. M. Kłosek-Dygas, B. J. Matkowsky, and Z. Schuss, to be published.
[10] A. M. Berezhkovskii, L. M. Berezhkovskii, and V. Yu. Zitserman, Chem. Phys. *30*, 55 (1989); Chem. Phys. Lett. *158*, 369 (1989).
[11] A. M. Berezhkovskii and V. Yu. Zitserman, to be published.
[12] N. Agmon and R. Kosloff, J. Phys. Chem. *91*, 1988 (1987). Further numerical work on this model is presented in the paper by Agmon and Rabinovich in this volume.
[13] C. Gehrke, J. Schröder, D. Schwartzer, J. Troe, and F. Voss, J. Chem. Phys. *92*, 4805 (1990).
[14] A. D. Kaufman and K. B. Whaley, J. Chem. Phys. *90*, 2758 (1989).
[15] M. D. Feit, J. A. Fleck, Jr., and Steiger, J. Comput. Phys. *47*, 412 (1982); M. D. Feit and J. A. Fleck, Jr., J. Chem. Phys. *78*, 301 (1983).
[16] a) D. Kosloff and R. Kosloff, J. Comput. Phys. *53*, 35 (1983); b) H. Tal Ezer and R. Kosloff, J. Chem. Phys. *81*, 3967 (1984). c) Review see: R. Kosloff, J. Phys. Chem. *68*, 2959 (1978).
[17] N. G. van Kampen, J. Stat. Phys. *17*, 71 (1977).
[18] N. G. van Kampen, Stochastic Processes in Physics and Chemistry, North Holland, Amsterdam 1981.
[19] D. Chandler, Introduction to Modern Statistical Mechanics, Oxford University Press, Oxford 1987.
[20] H. Risken, The Fokker-Planck Equation, Springer-Verlag, Berlin 1984.
[21] D. Chandler, J. Chem. Phys. *68*, 2959 (1978).
[22] H. A. Kramers, Physica *7*, 284 (1940).
[23] H. C. Brinkman, Physica *22*, 149 (1956); G. H. Vineyard, J. Phys. Chem. Solid *3*, 121 (1957); R. Landauer and J. A. Swanson, Phys. Rev. *121*, 1668 (1961); H. R. Glyde, Rev. Mod. Phys. *39*, 373 (1967); J. S. Langer, Phys. Rev. Lett. *21*, 973 (1968) and A.. Phys. (NY) *54*, 258 (1979); Z. Schuss, Theory and Application of Stochastic Differential Equations, Wiley, New York 1980; R. F. Grote and J. T. Hynes, J. Chem. Phys. *74*, 4465 (1981) and ibid. *75*, 2191 (1981).

Presented at the Discussion Meeting of the Deutsche Bunsen-Gesellschaft für Physikalische Chemie "Rate Processes in Dissipative Systems: 50 Years after Kramers" in Tutzing, September 10–13, 1990

E 7490